

## Rapid Roughening in Thin Film Growth of an Organic Semiconductor (Diindenoperylene)

A. C. Dürr,<sup>1,\*</sup> F. Schreiber,<sup>1,2,†</sup> K. A. Ritley,<sup>1</sup> V. Kruppa,<sup>1</sup> J. Krug,<sup>3</sup> H. Dosch,<sup>1,2</sup> and B. Struth<sup>4</sup>

<sup>1</sup>Max-Planck-Institut für Metallforschung, Heisenbergstraße 3, 70569 Stuttgart, Germany

<sup>2</sup>Universität Stuttgart, Pfaffenwaldring 57, 70550 Stuttgart, Germany

<sup>3</sup>Fachbereich Physik, Universität Essen, 45117 Essen, Germany

<sup>4</sup>ESRF, BP 220, F-38043 Grenoble CEDEX, France

(Received 5 July 2002; published 8 January 2003)

The scaling exponents  $\alpha$ ,  $\beta$ , and  $1/z$  in thin films of the organic molecule diindenoperylene deposited on SiO<sub>2</sub> under UHV conditions are determined. Atomic-force microscopy, x-ray reflectivity, and diffuse x-ray scattering were employed. The surface width displays power law scaling over more than 2 orders of magnitude in film thickness. We obtained  $\alpha = 0.684 \pm 0.06$ ,  $\beta = 0.748 \pm 0.05$ , and  $1/z = 0.92 \pm 0.20$ . The derived exponents point to an unusually rapid growth of vertical roughness and lateral correlations. We suggest that they could be related to lateral inhomogeneities arising from the formation of grain boundaries between tilt domains in the early stages of growth.

DOI: 10.1103/PhysRevLett.90.016104

PACS numbers: 68.55.-a, 81.15.Aa, 81.15.Kk

Organic semiconductors are in the focus of increasing research activity due to their potential for electronic and optoelectronic applications. In organic electronic devices, thin films of specific organic semiconductors serve as active layer. Recently, it has been shown that the structure (and as a consequence the physical properties) of thin organic layers depends crucially on the conditions employed during growth [1]. Hence, knowledge of the growth mechanism is necessary to predict structural features and to allow for a better control of the structural order.

In the past two decades, a theoretical framework was established which relates thin film growth mechanisms to a set of scaling exponents describing the dependence of the surface roughness on film thickness and lateral length scale. Much effort has been spent to theoretically predict scaling exponents for certain growth models, as well as to determine them experimentally for a large variety of thin film systems [2,3]. However, detailed studies that independently measure several scaling exponents with complementary techniques are rare, and the growth of organic thin films, and, in particular, the deposition of small molecules under ultrahigh vacuum (UHV) conditions, has been addressed only in a few cases [4–6]. In this Letter, we report the first measurements of scaling exponents for highly ordered thin films of the organic semiconductor diindenoperylene (DIP) deposited onto atomically smooth SiO<sub>2</sub> substrates in UHV, employing noncontact atomic-force microscopy (NC-AFM), specular x-ray reflectivity (XRR), and diffuse x-ray scattering (DXRS). Our key finding is that these films display an unusually rapid growth of vertical roughness and lateral correlations. A survey of the available growth scenarios suggests a novel roughening mechanism related to grain boundaries between tilt domains, which are a common feature of many organic thin films.

The scaling theory of growth-induced surface roughness is based on the behavior of the height difference correlation function (HDCF), the mean square height difference  $g(R) = \langle [h(x, y) - h(x', y')]^2 \rangle$  of pairs of points laterally separated by  $R = \sqrt{(x - x')^2 + (y - y')^2}$ . The HDCF can be evaluated from real space images by a spatial average over one or several regions, which should be much larger than  $R$  to avoid edge effects. The HDCF displays distinct behaviors for  $R \ll \xi$  and  $R \gg \xi$ , where  $\xi$  denotes the correlation length. For  $R \ll \xi$ , one expects a power law increase as  $g(R) \approx a^2 R^{2\alpha}$ , where  $\alpha$  is the static roughness exponent and  $a$  is a measure of the typical surface slope. For  $R \gg \xi$ , the heights at distance  $R$  become uncorrelated; hence,  $g(R)$  saturates at the value  $g(R \gg \xi) = 2\sigma^2$ , where the surface roughness  $\sigma = \langle (h - \langle h \rangle)^2 \rangle^{1/2}$  is the standard deviation of the film height. The three parameters  $\sigma$ ,  $\xi$ , and  $a$  evolve with film thickness  $D$  according to the power laws  $\sigma \sim D^\beta$ ,  $\xi \sim D^{1/z}$ , and  $a \sim D^\lambda$ , defining the growth exponent  $\beta$ , the dynamic exponent  $z$ , and the steepening exponent  $\lambda$ . Assuming that the regimes  $R \ll \xi$  and  $R \gg \xi$  are connected through a scaling form  $g(R) = 2\sigma^2 \tilde{g}(R/\xi)$ , it follows that the scaling exponents are related by  $\beta = \alpha/z + \lambda$ . For  $\lambda = 0$  (no steepening), one has  $\beta = \alpha/z$ . Scaling with  $\lambda > 0$  is referred to as *anomalous* [3].

The roughness parameters can also be determined by analyzing the DXRS intensity. Given that  $\sigma_{\text{substrate}} \approx 1.7 \text{ \AA} \ll \sigma_{\text{film}}$ , the latter can be written as [7]

$$I(q_x) \propto \int_0^\infty (\exp\{|q_z|^2[\sigma^2 - g(R)/2]\} - 1) e^{iq_x R} dR, \quad (1)$$

where  $q_x$  and  $q_z$  are the momentum transfers parallel and normal to the surface, respectively. To evaluate the integral (1), the scaling function  $\tilde{g}(x) = 1 - \exp(-x^{2\alpha})$  is commonly used [7]. This allows one to fit the DXRS

intensity of a given sample with only two free parameters,  $\alpha$  and  $\xi$ , since  $\sigma$  can be fixed by the analysis of the XRR.

DIP is a planar molecule with the extensions  $\approx 18.4 \text{ \AA} \times 7 \text{ \AA}$  [Fig. 1(a)]. DIP films with  $69 \text{ \AA} \leq D \leq 9000 \text{ \AA}$  were prepared on oxidized ( $4000 \text{ \AA}$ ) Si(100) substrates at  $T_{\text{substrate}} = 145 \pm 5 \text{ }^\circ\text{C}$  and at a deposition rate of  $12 \pm 3 \text{ \AA/min}$  under UHV conditions ( $p_{\text{base}} \leq 5 \times 10^{-10} \text{ mbar}$ ). Prepared under these conditions, the molecules adsorb on  $\text{SiO}_2$  standing essentially upright (lattice constant  $d_{\text{DIP}} \approx 16.55 \text{ \AA}$  [8]) with a tilt angle  $\phi$  presumably around  $15^\circ$ – $20^\circ$ , which gives rise to tilt domains [Fig. 1(a)].

For most of the samples, NC-AFM measurements were carried out immediately after deposition on several spots of the sample in an analysis chamber attached to the preparation chamber without breaking the UHV (OMICRON-AFM, scan range  $L \leq 5 \text{ }\mu\text{m}$ ). Subse-

quently,  $g(R)$  was calculated for each spot and the resulting bunch of HDCF's for each sample was averaged. The slope of a linear fit to the region  $R \ll \xi$  in a log-log-plot of the averaged function  $g(R)$  provides an estimate of  $2\alpha$ . The thickest sample ( $9000 \text{ \AA}$ ) has been measured in a DI Nanoscope III AFM in air due to its larger lateral scanning range (up to  $16 \text{ }\mu\text{m}$ ).

X-ray measurements were carried out at beam line ID10B at the ESRF in Grenoble, France, employing a wavelength  $\lambda = 1.563(2) \text{ \AA}$ . The radial resolution was  $0.007^\circ$  and the beam divergence behind the optics was better than  $0.003^\circ$ . Thus, the transversal coherence length of the beam is  $\chi_{\text{trans},0} > 15000 \text{ \AA}$  for normal incidence. The roughness  $\sigma$  of the samples with  $D \leq 1100 \text{ \AA}$  was characterized by analyzing their XRR [7].

DXRS data were recorded at several scattering vectors  $2\Theta \leq 2^\circ$  in rocking scans, where the incident angle,  $\alpha_i$ , is

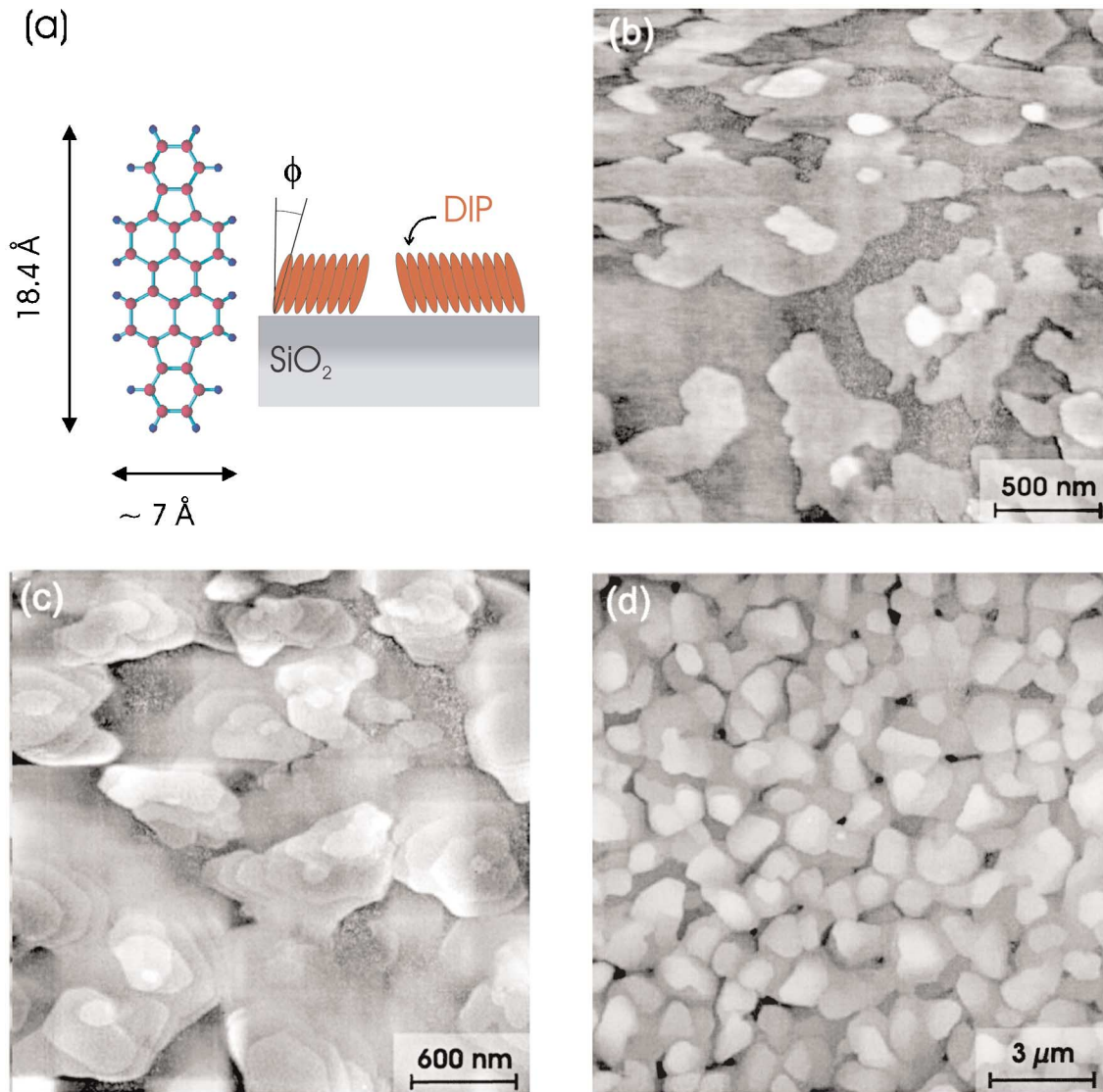


FIG. 1 (color). The molecule DIP ( $\text{C}_{32}\text{H}_{16}$ ) and a sketch illustrating the formation of tilt domains (a). NC-AFM images for several films:  $D = 126 \text{ \AA}$  (b),  $D = 1100 \text{ \AA}$  (c),  $D = 9000 \text{ \AA}$  (d).

varied while  $2\Theta = \alpha_i + \alpha_f$  is kept constant ( $\alpha_f$  denotes the exit angle). The data were fitted according to (1) with  $\sigma$  taken from the analysis of the XRR data. The resulting values for  $\alpha$  and  $\xi$  of the different positions in  $2\Theta$  for each sample were averaged.

Figures 1(b)–1(d) display NC-AFM images of samples with different  $D$ . Figure 2 shows a log-log plot of the averaged HDCF for five samples. An average value of  $\alpha_{\text{AFM}} = 0.628 \pm 0.05$  has been determined.

The roughness exponent as well as the inverse dynamic scaling exponent  $1/z$  have additionally been determined by fits of diffuse x-ray scattering in rocking-scan geometry as described above. Figure 3(a) shows a typical rocking scan and a fit to the data. The main plot of Fig. 3 displays a log-log plot of the correlation length  $\xi$  as a function of the film thickness. A linear fit to these data gives  $1/z = 0.92 \pm 0.20$ . An average of  $\alpha_{\text{DXRS}} = 0.74 \pm 0.07$  was obtained, which is slightly larger than  $\alpha_{\text{AFM}}$ . The average roughness exponent defined by  $\tilde{\alpha} = (\alpha_{\text{AFM}} + \alpha_{\text{DXRS}})/2$  is then given by  $\tilde{\alpha} = 0.684 \pm 0.06$ .

Figure 4 shows a log-log plot of  $\sigma$  as a function of  $D$  as derived from the analysis of XRR data for  $D \leq 1100$  Å and from the analysis of NC-AFM images for  $D = 9000$  Å. The solid line is a linear fit to the data, and we obtained  $\beta = 0.748 \pm 0.05$ . Note that the inspected range of film thickness  $D$  covers more than 2 orders of magnitude, and that no systematic deviation from the power law can be detected.

Using the quoted values for  $\alpha$ ,  $\beta$ , and  $z$ , the steepening exponent  $\lambda$  is estimated to be 0.17 (0.07) for  $\alpha = \alpha_{\text{AFM}}$  ( $\alpha = \alpha_{\text{DXRS}}$ ). This suggests that some steepening is present, but that the effect is rather weak, consistent with the modest upward shift of the HDCF's displayed in Fig. 2 with increasing film thickness.

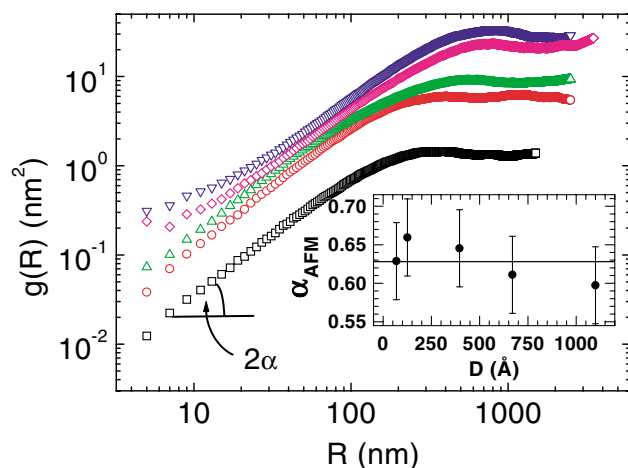


FIG. 2 (color). Averaged  $g(R)$  for five samples with various  $D$  ( $\square = 69$  Å,  $\circ = 126$  Å,  $\triangle = 396$  Å,  $\nabla = 670$  Å,  $\diamond = 1100$  Å). The inset displays  $\alpha$  obtained by fitting the linear part of  $g(R)$  as a function of  $D$ ; the horizontal line denotes the average of  $\alpha$ .

Two main mechanisms for growth-induced surface roughening have been described in the literature. In *kinetic roughening*, the roughness arises from the competition between the shot noise and surface smoothing through surface diffusion, desorption, and related processes. The resulting morphology is self-affine, showing statistical scale invariance on length scales below the correlation length  $\xi$ . In contrast, in *mound growth* a pattern with a well-defined characteristic length scale develops as a consequence of a morphological instability, which is usually associated with reduced interlayer transport. The scaling picture sketched above applies in both cases, with the mound size playing the role of the correlation length  $\xi$  in the second scenario. The two scenarios differ in the shape of the HDCF, which should display clear oscillations in the case of mound growth [3].

The estimates for  $\alpha$  obtained in this work are consistent with kinetic roughening in the conserved Kardar-Parisi-Zhang (KPZ) universality class, for which  $\alpha \approx 2/3$  [3]. Similar values are commonly reported for inorganic films [2]. For mounds  $\alpha = 1$  asymptotically, but in practice much lower values may occur [9]. Hence, a case of noisy mound growth also cannot be ruled out for the DIP films. By visual inspection, Figs. 1(b) and 1(c) suggest an essentially random appearance of the surface, while Fig. 1(d) resembles a mound pattern (compare to Fig. 1 of [9]). However, both scenarios have considerable difficulties in explaining the large values of  $1/z$  and  $\beta$ . For conserved KPZ growth,  $1/z \approx 0.3$  and  $\beta \approx 0.2$  due to the scaling relation [3]  $z = 2 + 2\alpha$ . For mound growth, large values of  $\beta$  up to  $\beta \approx 0.8$  have been observed in simulations [10], but this behavior is restricted to an intermediate regime associated with considerable

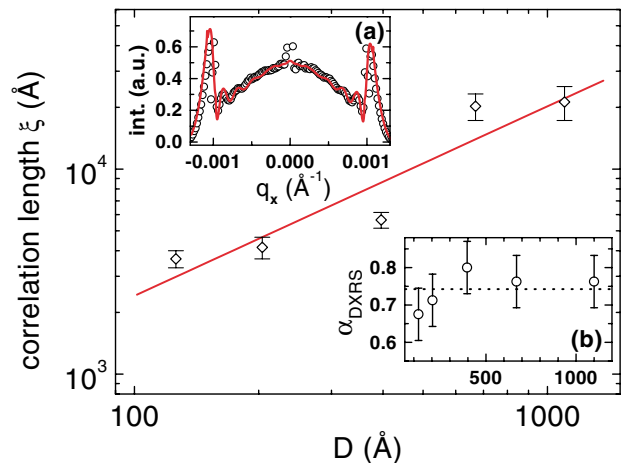


FIG. 3 (color). Log-log plot of  $\xi$  vs  $D$  as obtained by fits to rocking scans over the specular rod ( $\diamond$ ). The solid line is a linear fit to the data which gives  $1/z$ . Inset (a) displays a rocking scan ( $\circ$ ) and a fit (solid line) associated with the data for a DIP film with  $D = 396$  Å recorded at  $2\Theta = 1.5^\circ$ . Inset (b) displays the values of  $\alpha$  as obtained by fits to the rocking scans; the dotted line shows the average of  $\alpha$ .

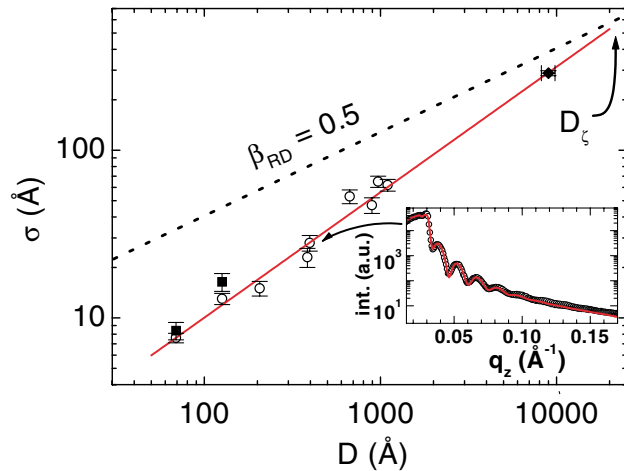


FIG. 4 (color). Log-log plot of  $\sigma$  vs  $D$  and a linear fit to the data which gives  $\beta = 0.748 \pm 0.05$ . For  $D \leq 1100$  Å, XRR was used to determine  $\sigma$  (○); see inset as a typical example for a sample with  $D = 396$  Å. For some samples  $\sigma$  was determined also by NC-AFM (■ = OMICRON, ◆ = DI). The dotted line with slope  $\beta_{RD} = 0.5$  corresponds to the random deposition limit  $\sigma_{RD} = d_{DIP}\sqrt{D/d_{DIP}}$ , which would be reached at  $D_\zeta$ .

steepening, where the dynamic exponent takes on a conventional value of  $1/z \approx 0.2-0.3$ .

Both in kinetic roughening and in mound growth, the random deposition (RD) limit  $\sigma_{RD} = d_{DIP}\sqrt{D/d_{DIP}}$  is expected to provide an absolute upper bound on  $\sigma$  [3]. This bound is attained if every particle remains on the height level where it was deposited [11]. Roughness beyond  $\sigma_{RD}$  can occur only if matter is transported to higher layers, which would require a thermodynamic driving force, as, e.g., in dewetting. We have no indication for such a thermodynamic instability in our films. Although the DIP data in Fig. 4 remain below  $\sigma_{RD}$  for all film thicknesses, the fact that we observe no deviation from the power law suggests that the scaling with  $\beta > 1/2$  will continue also beyond the thickness  $D_\zeta$  where the DIP roughness crosses the RD limit. *Rapid roughening*, in the sense of  $\beta > 1/2$  [3], has previously been reported for a number of systems [4,12–14], but no general mechanism has been identified.

At present, the only model which is consistent with the scaling exponents measured in this work involves random spatial inhomogeneities in the local growth rate, which are fixed during the growth process. It is plausible that, when certain regions of the surface persistently grow faster than others, the surface will roughen very rapidly. The quantitative analysis [15] shows that the roughness and the correlation length grow subballistically as  $\sigma \sim D/[\ln(D)]^\phi$ ,  $\xi \sim D/[\ln(D)]^\psi$ , where  $\phi, \psi \approx 2-3$ . Thus, asymptotically  $\alpha = \beta = 1/z = 1$ , but smaller effective exponents are measured; e.g.,  $\beta = 0.7-0.8$  and  $\alpha \approx 0.8$  for the one-dimensional models of [15].

We attribute these spatial inhomogeneities to the tilt domains of the film [Fig. 1(a)]. In analogy with the

epitaxial growth of inorganic films, one expects the formation of two-dimensional islands during the growth of the first monolayer [1]. The orientation of the molecules is fixed within each growing island, but different islands chose different in-plane orientations of the tilt vector. If the resulting two-dimensional grain boundaries which form during the coalescence of the first layer propagate to the subsequent layers, the growth rate at these grain boundaries is likely to differ from that on top of a crystalline DIP domain. This would in fact give rise to the observed rapid roughening phenomenon.

In conclusion, we have independently determined the three scaling exponents  $\alpha$ ,  $\beta$ , and  $1/z$  for highly ordered thin films of the organic semiconductor DIP deposited onto silicon-dioxide substrates under UHV conditions employing NC-AFM, specular x-ray reflectivity, and diffuse x-ray scattering in rocking-scan geometry. The large values of  $\beta$  and  $1/z$  show that DIP films grown under the employed deposition conditions belong to a class of systems which display the (largely unexplained) phenomenon of rapid roughening. We have tentatively attributed the behavior to lateral inhomogeneities, which could be associated with the orientational degrees of freedom of the DIP molecules. It would be highly desirable to investigate the early stages of DIP film growth by *in situ* AFM studies to independently test this scenario.

We thank V. Holý for helping to fit the DXRS data and U. Täffner for help in the AFM measurements. F. S. and J. K. acknowledge support from the DFG within the focus program “Organische Feldeffekt-Transistoren” and SFB 237, respectively.

\*Electronic address: Arndt.Duerr@mf.mpg.de

†New address: Physical and Theoretical Chemistry Laboratory, University of Oxford, South Parks Road, Oxford OX1 3QZ, England.

- [1] F.-J. Meyer zu Heringdorf *et al.*, Nature (London) **412**, 517 (2001).
- [2] J. Krim and G. Palasantzas, Int. J. Mod. Phys. B **9**, 599 (1995).
- [3] J. Krug, Adv. Phys. **46**, 139 (1997).
- [4] G.W. Collins *et al.*, Phys. Rev. Lett. **73**, 708 (1994).
- [5] F. Biscarini *et al.*, Phys. Rev. Lett. **78**, 2389 (1997).
- [6] Y.-P. Zhao *et al.*, Phys. Rev. Lett. **85**, 3229 (2000).
- [7] V. Holý, U. Pietsch, and T. Baumbach, *High-Resolution X-Ray Scattering From Thin Films and Multilayers* (Springer, Berlin, 1999).
- [8] A.C. Dürr *et al.*, Appl. Phys. Lett. **81**, 2276 (2002).
- [9] G. Lengel *et al.*, Phys. Rev. B **60**, R8469 (1999).
- [10] K. J. Caspersen *et al.*, Phys. Rev. B **65**, 193407 (2002).
- [11] M. Kalff *et al.*, Surf. Sci. **426**, L447 (1999).
- [12] K. Fang *et al.*, Phys. Rev. B **49**, 8331 (1994).
- [13] C.J. Lanczycki *et al.*, Phys. Rev. B **57**, 13132 (1998).
- [14] J.-P. Schlomka *et al.*, Appl. Phys. Lett. **76**, 2005 (2000).
- [15] J. Krug, Phys. Rev. Lett. **75**, 1795 (1995).